

Convolution Operations on Coding Metasurface for RCS Reduction

Tingting Shang, Jianping Zhao, and Juan Xu

School of Cyber Science and Engineering
Qufu Normal University, Qufu 273165, People's Republic of China
tingzi2046@163.com, zjp-wlx@163.com, xujuan125@163.com

Abstract – In this paper, a polarization conversion unit is designed as the coding unit. The units are arranged in a regular cross-arrangement. Convolution operation is composed of the Dirac-delta function and the principle of scattering-pattern shift. The Dirac-delta is optimized by generalized Snell's law and addition theorem. According to the convolution operations, the cross-arrangement pattern is shifted to multiple directions to reduce the backscattering field. Compared with regularly arranged metasurface, this method can reduce the radar cross section (RCS) of single station by at least 10 dB. Compared with the traditional intelligent optimization algorithm, this method provides a new route to reduce RCS by random distribution of elements.

Index Terms – Convolution operations, cross-arrangement pattern, polarization conversion, metasurface, principle of scattering-pattern shift, radar cross section, the Dirac-delta function.

I. INTRODUCTION

The reduction of radar cross section (RCS) is obtained by redirecting the backscattering waves to multiple directions. The research focus is using the optimization algorithm to realize random cell placement and ultra-wideband RCS reduction. In 2011, the generalized Snell's law was proposed by Yu. The abnormal reflection and refraction in the optical band were realized by introducing gradient phase into the metasurface. A "V" shaped element was designed and the gradient phase was adjusted by controlling its opening angle and rotation angle in [1]. In 2014, the concept of coding metasurface was first proposed by Professor Cui Tie Jun. He designed 1-bit and 2-bit coding metasurfaces in microwave band with rectangular patch structure, which can reduce RCS by more than 10 dB in 7.8–12 GHz and 7.5–15 GHz bands respectively in [2]. In 2017, Liu realized π phase difference of broadband by AMC unit in [3]. However, Su achieved π phase difference by adjusting size of square ring structure in ultra-wide frequency band. Particle swarm optimization (PSO) is used to optimize the arrangement sequence of cells, and finally multi-beam distribution with broadband RCS reduction

is obtained in [4]. In 2020, the programmable metasurface for multi-beam control using deep learning technology was proposed by Shan to reduce RCS in [5]. The random distribution of metasurface elements is realized by the optimization algorithm, which is time-consuming in programming and slow in running. The metasurface can be transformed from a regular metasurface to a random metasurface by shifting the regular metasurface scattering pattern to multiple directions. This convolution operation can not only avoid programming and iteration problems, but also achieve RCS reduction.

In this paper, the cross-arrangement matrix is added by the Dirac-delta function to realize the shift of scattering pattern. The function is optimized by using generalized Snell's law and addition theorem. The RCS is further reduced by shifting the cross-arrangement scattering pattern to multiple directions. Because the effect of RCS reduction by metal plate is poor, we choose to compare the metasurface which cross-arrangement scattering pattern is shifted to multiple directions with cross-arrangement metasurface with the same size. Finally, this metasurface achieves single station RCS reduction of more than 10 dB.

II. MATERIALS AND METHODS

A. Principle of scattering-pattern shift

The convolution theorem in Fourier transform describes the common multiplication of signals in time domain and the convolution of corresponding frequency spectrum in frequency domain.

$$f(t) \cdot g(t) \Leftrightarrow F(\omega) * G(\omega). \quad (1)$$

Equation (1) can be simplified as frequency-shift function when $G(\omega)$ becomes a Dirac-delta function, the equation (1) is rewritten as:

$$f(t) \cdot \exp(j\omega_0 t) \Leftrightarrow F(\omega) * \delta(\omega - \omega_0) = F(\omega - \omega_0). \quad (2)$$

Referring to the theory in [6], the electric field distribution on the coding metasurface and the scattering pattern in the far-field region are Fourier transform pairs. Which can connect the coding-pattern domain (in analogy to the time domain) with the scattering-pattern domain (in analogy to the frequency domain). As is mathematically expressed as:

$$e(x_\lambda) \cdot g(x_\lambda) \Leftrightarrow E(\sin \theta) * G(\sin \theta), \quad (3)$$

where x_λ is the electrical length, θ is the angle with respect to the normal direction. Equation (3) is rewritten into the form of the equation (2):

$$e(x_\lambda) \cdot \exp(jx_\lambda \sin \theta_0) \Leftrightarrow E(\sin \theta_0) * \delta(\sin \theta - \sin \theta_0) = E(\sin \theta - \sin \theta_0). \quad (4)$$

The multiplication of $e(x_\lambda)$ by a gradient sequence $\exp(jx_\lambda \sin \theta_0)$ is the multiplication of $\exp(j\varphi_1)$ by $\exp(j\varphi_2)$.

$$\exp(j\varphi_1) \cdot \exp(j\varphi_2) = \exp(j(\varphi_1 + \varphi_2)). \quad (5)$$

Taking $\varphi_1 = 0$ and $\varphi_2 = \pi$ in equation (5), it can be rewritten as equation (6). Selecting φ of $\exp(j\varphi)$ in equation (6), it can be abbreviated as equation (7).

$$\exp(j0) \cdot \exp(j\pi) = \exp(j(0 + \pi)) = \exp(j\pi). \quad (6)$$

$$0 + \pi = \pi. \quad (7)$$

Because 0 in the coding matrix represents $\varphi = 0$ and 1 represents $\varphi = \pi$, the coding matrix is associated with the phase of the unit.

$$0 + \pi = \pi \Leftrightarrow 0 + 1 = 1. \quad (8)$$

In fact the operation on the coding matrix is to operate on the phase distribution, so as to shift the scattering pattern. The above equations relate the coding matrix to the far-field pattern. As shown in Figure 1, the addition of coding matrix means the far-field pattern is shifted.

B. Optimization of dirac-delta function

To reduce RCS as much as possible, it is necessary to shift the cross-arrangement scattering pattern to more directions. In other words, the Dirac-delta function needs to be optimized. Beam steering is realized by generalized

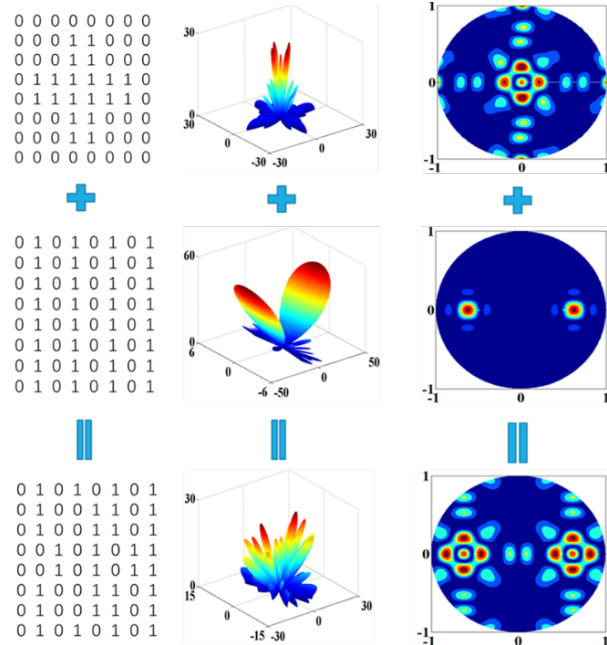


Fig. 1. Schematic diagram of scattering-pattern shift.

Snell’s law. Then, coding matrices are superimposed by addition theorem [7]. Therefore, a Dirac-delta function is generated that can be shifted to four directions, six directions, and more.

Taking Figure 2 as an example to introduce the generation of Dirac-delta function that shift the scatter pattern to four directions. When the coding sequence of the coding metasurface is 0101... / 0000... or 0000... / 0101..., it can be obtained that the metasurface has two scattering beams according to the generalized Snell’s law. Using the addition coding theorem, the coding sequence 0101... / 0101... can be obtained. It can integrate the far-field scattering characteristics of coding sequence 0101... / 0000... and coding sequence 0000... / 0101... to generate four scattering beams. To better visualize the direction of scattering beam, Figure 2 gives the corresponding 2D scattering pattern in a polar coordinate system. From the 2D scattering pattern, four lighter spots represent not only the four main lobes but also the four directional points of the Dirac-delta function that shift the scattering pattern to four directions.

Based on the above theory, the Dirac-delta function is selected in Figure 2. The cross-arrangement scattering pattern is shifted to four directions by the

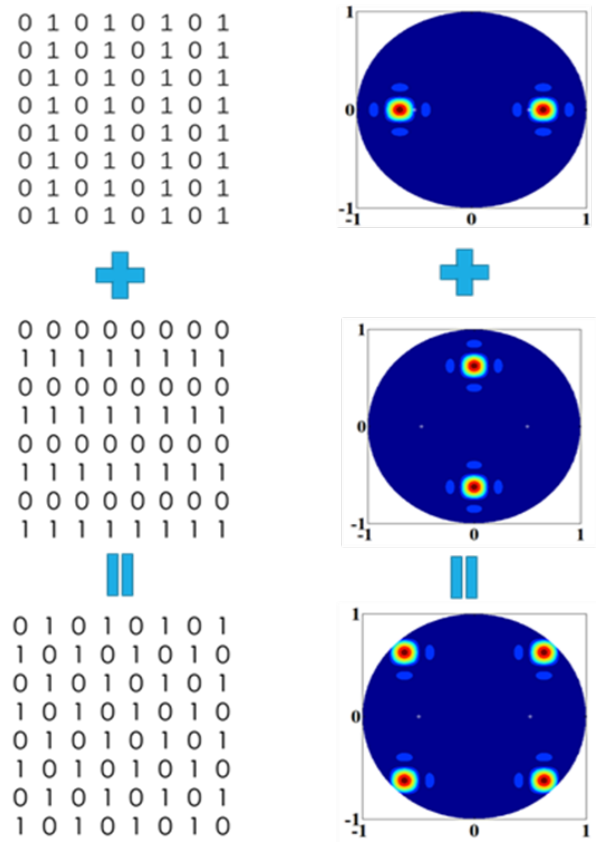
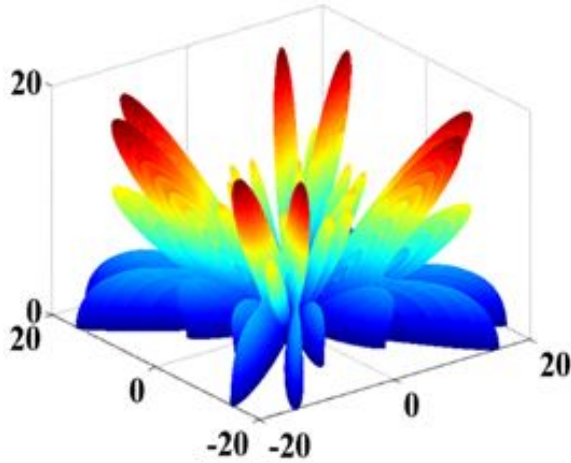
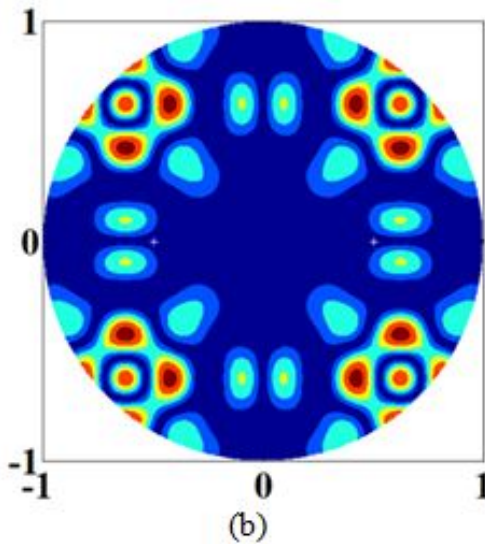


Fig. 2. Schematic diagram of addition theorem.



(a)



(b)

Fig. 3. Pattern of metasurface which cross-arrangement scattering pattern is shifted to four directions. (a) 3D view. (b) 2D polar view.

principle of scattering-pattern shift. In an ideal situation, the cross-arrangement scattering pattern is shifted to four directions in 3D pattern in Figure 3 (a) and the energy distribution in 2D polar coordinates in Figure 3 (b).

III. PERFORMANCE CHARACTERIZATION

A. Design of the metasurface unit

In order to better verify the above theory, a polarization conversion [8] metasurface element is proposed as shown in Figure 4 (a). The unit structure includes three layers, which are metal floor, dielectric substrate, and structural layer from bottom to top. Rogers 5880 substrate is used as the dielectric plate. The relative dielec-

Table 1: Size parameter of the unit

Variables	l	k	d	c	w	h
Size(mm)	4	0.52	4.3	0.9	0.3	1.75

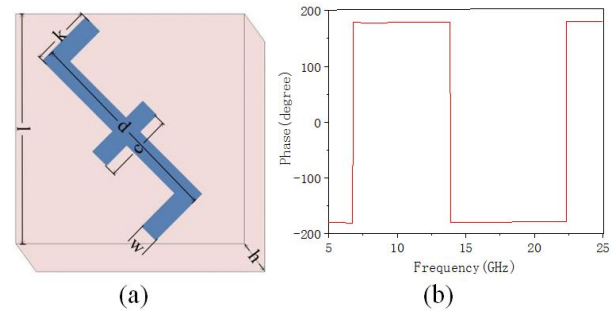


Fig. 4. (a) Structure diagram of polarization conversion unit. (b) Cross-polarization phase difference.

tric constant is 2.2 and the loss tangent angle is 0.0009. The size parameters are shown in Table 1.

The corresponding mirror unit can be obtained by mirroring the unit. The unit realizes wave cancellation by converting incident electromagnetic wave (EM) into cross-polarization component. As shown in Figure 4(b), because the cross polarization [9] phase difference between polarization conversion unit and its mirror unit is π , it is regarded as coding unit ("0" unit, "1" unit).

B. Optimization of unit arrangement

According to the coding matrix, the coding units are arranged in a cross-arrangement and metasurface which the cross-arrangement scattering pattern is shifted to two, four, or six directions. The metasurface is composed of 8×8 super-units with dimensions of $64 \text{ mm} \times 64 \text{ mm}$, where the super-unit is composed of 2×2 anisotropic unit cells. The metasurface is simulated and analyzed by commercial simulation software HFSS. Figures 5 and 6

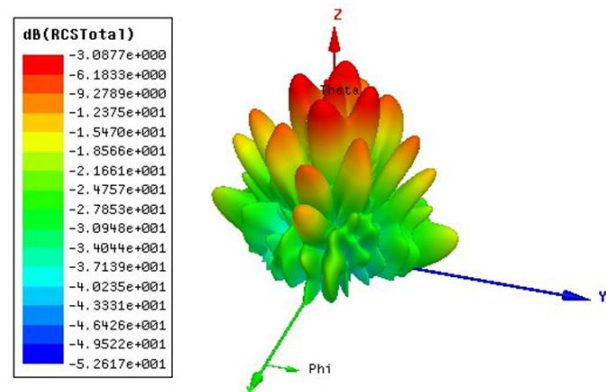


Fig. 5. The cross-arrangement scattering pattern at $f = 32 \text{ GHz}$.

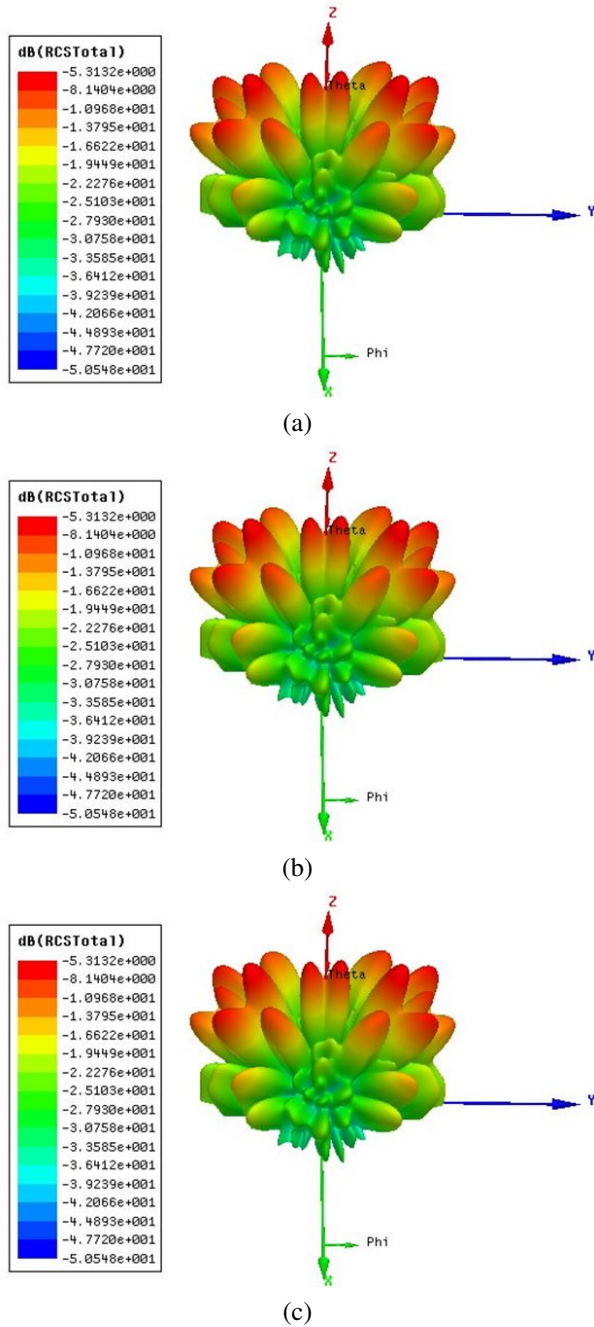


Fig. 6. The cross-arrangement scattering patterns are shifted to multiple directions at $f = 32\text{GHz}$.

show the scattering pattern at $f = 32\text{GHz}$ when plane waves are incident vertically. The cross-arrangement scattering patterns is shown in Figure 5. The cross-arrangement scattering patterns are shifted to two directions in Figure 6 (a), four directions in Figure 6 (b), and six directions in Figure 6 (c). With the increase of shift direction, the energy distribution is more uniform. The incident electromagnetic energy is scattered

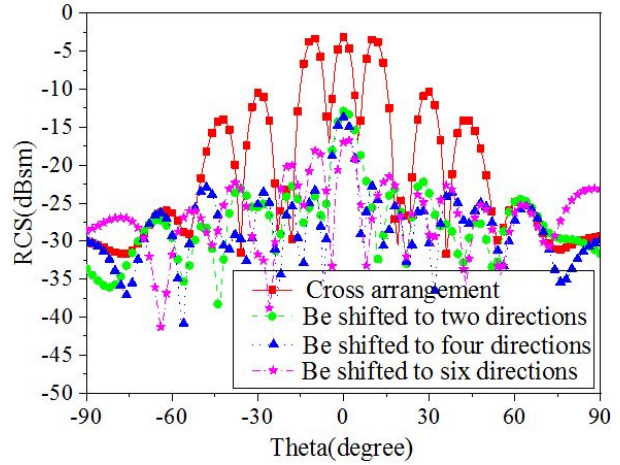


Fig. 7. 2D far-field scattering pattern plotted in y-z plane.

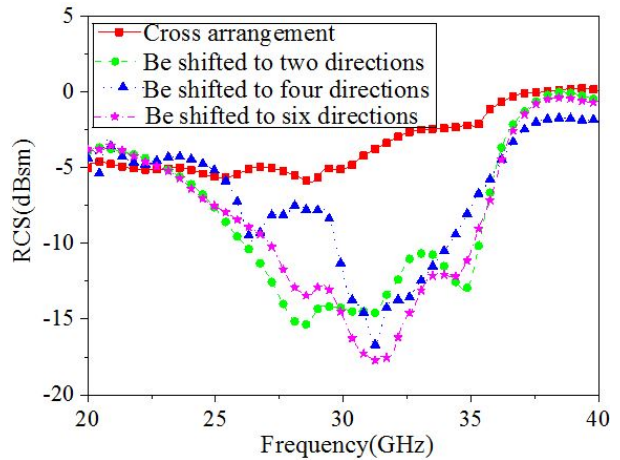


Fig. 8. The simulation results of RCS over a wide frequency range from 20 to 40 GHz.

in all directions after being reflected by the metasurface. According to the energy conservation theorem, the energy of each beam is very low, so the RCS in the vertical direction is obviously reduced. Figure 7 also proved that with the increase of the shift direction, the RCS in vertical direction decreases gradually.

In order to compare the RCS reduction of four electromagnetic metasurface more intuitively, Figure 8 shows the graph of single-station RCS change in 20–40 GHz band. The RCS of the metasurface which cross-arrangement scattering pattern is shifted to multiple directions is lower than the cross-arrangement metasurface. As the shift direction increases, so does the RCS reduction.

Compared with the cross-arrangement, the RCS reduction of the designed metasurfaces are illustrated in Figure 9. The metasurface is an array formed by the

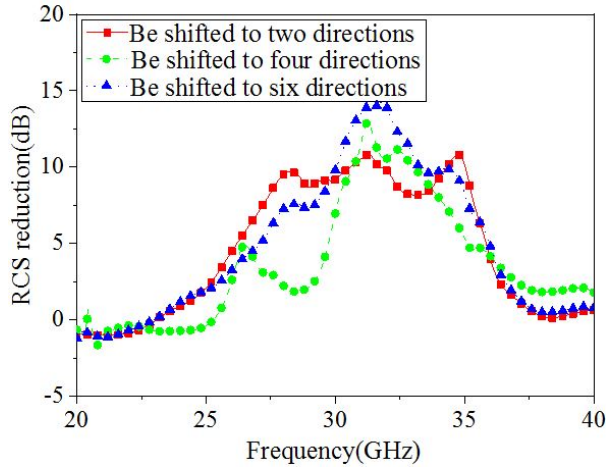


Fig. 9. Simulation results of RCS reduction.

cross-arrangement scattering pattern shifting to multiple directions. It shows that RCS reduction increases with the increase of the shifted direction of scattering pattern. Therefore, RCS reduction can be realized by designing the metasurface which regular arrangement scattering pattern is shifted to multiple directions. The more the shift direction, the greater the degree of RCS reduction.

IV. EXPERIMENTAL VERIFICATION

A prototype measuring $64 \text{ mm} \times 64 \text{ mm}$ was fabricated using printed circuit board technology to verify the RCS reduction characteristics of the metasurface which regular arrangement scattering pattern is shifted to six directions, as shown in Figure 10.



Fig. 10. Photographic view of fabricated sample.

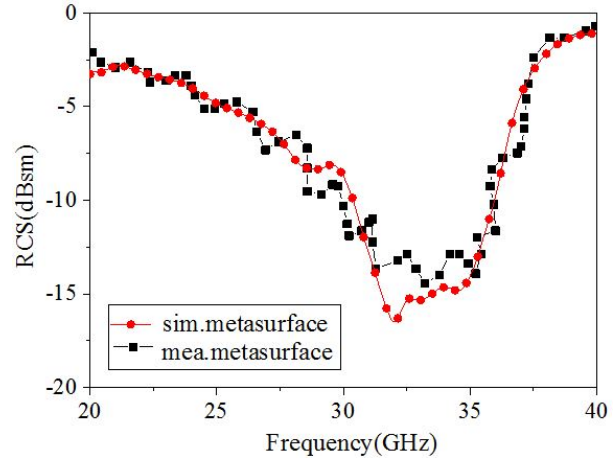


Fig. 11. Comparison of single-station RCS results of metasurface under normal incident of electromagnetic wave.

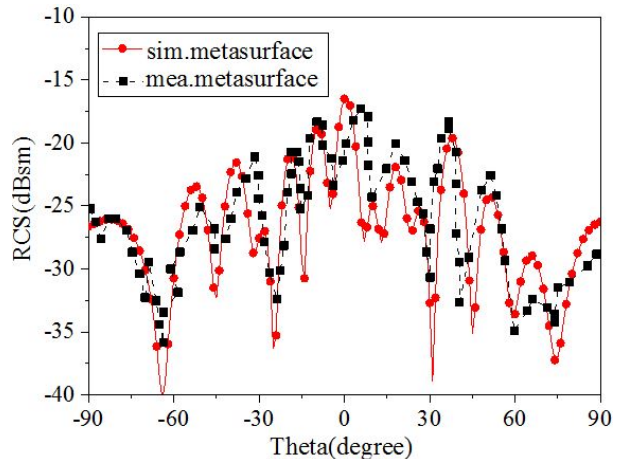


Fig. 12. Comparison of 2D far-field scattering pattern of metasurface under normal incident of electromagnetic wave.

The measurement was carried out in a microwave darkroom using the free space method. When the electromagnetic wave is normal incident, the characteristics of the single-station RCS of the metasurface changing with frequency are shown in Figure 11. As expected, the measured single-station RCS results matched well with the simulation results. And the measured RCS results in the vertical direction is also matched well with the simulation results in Figure 12. Of course, there are some errors within the acceptance range, which can be attributed to the following two reasons: (1) the incident wave in the simulation process is an ideal plane wave, while the plane incident wave in the actual measurement is approximately equivalent to the far-field radiation of

the horn antenna; (2) manufacturing tolerances in physical processing and inevitable deviations of naked eyes in measurement.

V. CONCLUSION

In this paper, a polarization conversion unit is designed, which is used as the coding unit because the phase difference between the polarization conversion unit and its mirror unit is π . Dirac-delta function is selected by using generalized Snell's law and addition theorem. Then the pattern is shifted to different directions by convolution theorem of Fourier transform. Finally, the radar cross section is reduced. The simulation results show that the metasurface which regular cross-arrangement scattering pattern is shifted to multiple directions can reduce RCS more effectively.

ACKNOWLEDGMENT

This work was supported in part by the National Natural Science Foundation of China (61701278).

REFERENCES

- [1] Nanfang Yu, P. Genevet, M. A. Kats, F. Aieta, J.-P. Tetienne, F. Capasso, and Z. Gaburro, "Light propagation with phase discontinuities: generalized laws of reflection and refraction," *Science*, vol. 33, pp. 333-337, 21 Oct. 2011.
- [2] Tie-Jun Cui, Mei-Qing Qi, Xiang Wan, Jie Zhao, and Qiang Cheng, "Coding metamaterials, digital metamaterials and programmable metamaterials," *Light: Sci. Appl.*, vol. 3, pp. 1-9, Sep. 2014.
- [3] Xiao Liu, Jun Gao, Li-Ming Xu, Xiang-Yu Cao, Yi Zhao, and Si-Jia Li, "A coding diffuse metasurface for RCS reduction," *IEEE Antennas and Wireless Propagation Letters*, vol. 16, pp. 724-727, Apr. 2017.
- [4] Jian-Xuan Su, Yao Lu, and Zeng-Rui Li, "Ultra-wideband Metasurface for Radar Cross Section Reduction," *ACES Conference*, pp. 1-2, 2017.
- [5] Tao Shan, Xiao-Tian Pan, and Mao-Kun Li, Shen-Heng Xu, and Fan Yang, "Coding programmable metasurfaces based on deep learning techniques," *IEEE Journal on Emerging and Selected Topics in Circuits and Systems*, vol. 10, no. 1, pp. 114-125, Mar. 2020.
- [6] Liu Shuo, Tie-Jun Cui, and Zhang Lei, "Metasurfaces: convolution operations on coding metasurface to reach flexible and continuous controls of terahertz beams," *Advanced Science*, pp. 1-12, Mar. 2016.
- [7] Rui-Yuan Wu, Chuan-Bo Shi, Shuo Liu, Wei Wu, and Tie-Jun Cui, "Addition theorem for digital coding metamaterials," *Advanced Optical Materials*, pp. 1-10, Jun. 2018.
- [8] Brian A. Lail and Kyu Y. Han, "Low-profile, broadband polarization converting surface ground planes for antenna polarization diversity," *Applied Computational Electromagnetics Society (ACES) Journal*, vol. 25, no. 1, pp. 54-60, Jan. 2010.
- [9] J. Su, C. Kong, Z. Li, X. Yuan, and Y. L. Yang, "Ultra-wideband and polarization conversion metasurface," *Applied Computational Electromagnetics Society (ACES) Journal*, vol. 32, no. 6, pp. 524-530, Jun. 2017.



Tingting Shang was born in Liaocheng, Shandong Province, China in 1996. She obtained her B.S. degree in engineering from Jining University, China, in 2019. In the same year, she was admitted to QuFu Normal University and became a graduate student.

Her research interest includes the design and optimization of electromagnetic metasurface.



Jianping Zhao was born in Heze, Shandong Province, China in 1964. He received his B.S. degree in physics from QuFu Normal University Qufu, China, in 1985. In 1988, he studied in Wuhan University for master's degree in radio and information engineering.

Since 1985, he has been working at QuFu Normal University. He was promoted to associate professor in 1997 and professor in 2002. Since 1992, he has been the director of the Radio Teaching and Research Section. He has been engaged in application of electronic technology and scientific research in communication and information system of electronic information engineering and communication engineering.



Juan Xu was born in Jining, Shandong Province, China, in 1982. She received her Ph.D. degree in electronic science and technology from Nanjing University of Science and Technology, Nanjing, China, in 2016. Since 2016, she has been working at QuFu Normal University.

She has been an associate professor since 2019.

Her research interests include simulation, design and experimental measurement of new high performance RF, microwave and millimeter wave passive devices, antennas, and antenna arrays.